Ab initio localized basis set study of structural parameters and elastic properties of HfO_2 polymorphs

2005 J. Phys.: Condens. Matter 17 5795

(http://iopscience.iop.org/0953-8984/17/37/015)

INSTITUTE OF PHYSICS PUBLISHING JOURNAL OF PHYSICS: CONDENSED MATTER

J. Phys.: Condens. Matter **17** (2005) 5795–5811 doi:10.1088/0953-8984/17/37/015

Ab initio localized basis set study of structural parameters and elastic properties of HfO_2 polymorphs

M A Caravaca[1] **and R A Casali**[2]

[1] Facultad de Ingenieria, Universidad Nacional del Nordeste, Avenida Las Heras 727, 3500-Resistencia, Argentina
[2] Facultad de Ciencias Exactas y Naturales y Agrimensura, Universidad Nacional del Nordeste, Avenida Libertad, 5600-Corrientes, Argentina

E-mail: mac@ing.unne.edu.ar

Received 19 May 2005, in final form 4 August 2005
Published 2 September 2005
Online at stacks.iop.org/JPhysCM/17/5795

Abstract

The SIESTA approach based on pseudopotentials and a localized basis set is used to calculate the electronic, elastic and equilibrium properties of $P2_1/c$, $Pbca$, $Pnma$, $Fm3m$, $P4_2nmc$ and $Pa3$ phases of HfO_2. Using separable Troullier–Martins norm-conserving pseudopotentials which include partial core corrections for Hf, we tested important physical properties as a function of the basis set size, grid size and cut-off ratio of the pseudo-atomic orbitals (PAOs).

We found that calculations in this oxide with the LDA approach and using a minimal basis set (simple zeta, SZ) improve calculated phase transition pressures with respect to the double-zeta basis set and LDA (DZ–LDA), and show similar accuracy to that determined with the PPPW and GGA approach. Still, the equilibrium volumes and structural properties calculated with SZ–LDA compare better with experiments than the GGA approach.

The bandgaps and elastic and structural properties calculated with DZ–LDA are accurate in agreement with previous state of the art *ab initio* calculations and experimental evidence and cannot be improved with a polarized basis set. These calculated properties show low sensitivity to the PAO localization parameter range between 40 and 100 meV. However, this is not true for the relative energy, which improves upon decrease of the mentioned parameter. We found a non-linear behaviour in the lattice parameters with pressure in the $P2_1/c$ phase, showing a discontinuity of the derivative of the a lattice parameter with respect to external pressure, as found in experiments.

The common enthalpy values calculated with the minimal basis set give pressure transitions of 3.3 and 10.8 GPa for $P2_1/c \rightarrow Pbca$ and $Pbca \rightarrow Pnma$, respectively, in accordance with different high pressure experimental values.

1. Introduction

The improvement in the operation of future MOSFETs requires a systematic reduction in the dimensions of the device. In the construction of the gate oxides, SiO_2 has been the most common material in the last 30 years up to the present. However, its low dielectric constant and the electrical losses due to tunnelling effects certainly are the main limitation in their future usage in sub-micrometric devices.

Refractory oxides play an important role as substitute materials and have attracted considerable attention due to their good dielectric properties, structural stability, layer bandgap and simple crystalline structures. For instance, electric measurements for HfO_2 deposited on SI substrate indicate a decrease of three to four orders of magnitude of the leakage current when it is compared with the equivalent thickness of SiO_2 films [1].

A dense layer of HfO_2 with good hardness can be deposited on Si[100] wafers by electron beam evaporation or sputtering and have good electrical and structural stability [2]. These properties, combined with others like high refraction index ($n = 2.2$), high dielectric constant ($n = 30$) and high hardness, show that it is a good candidate to be used not only as a high-k gate dielectric but for optical lens coating for the range from near UV (below 300 nm) to far infra-red, IR (10 μm) [2, 3]. At room temperature and pressure, hafnia is found in isostructural zirconia phases with the MO_2 formula, in which the metal ion M is seven coordinated. Structural similarity at ambient pressure between HfO_2 and ZrO_2 are customarily attributed to the lanthanide contraction. This effect shows (by x-ray diffraction) that the size of the trivalent rare earth ions progressively decreases as the atomic number rise. As a consequence, Hf and Zr show similar atomic size.

The phase diagram near room temperature of HfO_2 and ZrO_2 at pressures in excess of 70 GPa has been studied through angle-dispersive Raman spectroscopy and with energy-dispersive synchrotron x-ray diffraction [4]. In particular the HfO_2 undergoes phase transitions to denser structures in the following sequence: $P2_1/c$ (monoclinic (MI)) $\rightarrow$ $Pbcm$ ($Pbca$, orthorhombic (OI)) $\rightarrow$ $Pnma$ (orthorhombic (OII)), named cotunnite [5]. The phase OII has been confirmed to quench at pressures in excess of 30 GPa [6].

The only present phase at room temperature in compressed samples from 70 GPa, decompressed to 0 GPa and then compressed up to 30 GPa is cotunnite [4]. The quenched phases are: (a) about 13% denser than the normal one, (b) optically transparent, (c) stable at ambient condition, (d) of very low compressibility as indicated by their measured bulk modulus (340 GPa) [4].

At high temperature and normal pressure conditions, pure HfO_2 has three polymorphs: the cubic fluorite structure (space group $Fm3m$) stable above 2640 K, the tetragonal structure ($P4_2nmc$) stable between 1400 and 2640 K, and the monoclinic structure ($P2_1/c$) stable below 1400 K. Since the discovery in the mid-1970s of a transformation toughening in ZrO_2, a considerable effort has been devoted to search this transformation in other compounds. On the basis that HfO_2 exhibits similar crystal structure to ZrO_2 and although its tetragonal to monoclinic transformation temperature is approximately 700 K higher than that for ZrO_2, it has been suggested that similar high temperature transformation toughening could be possible in hafnia ceramics (HTCs). The evidence collected for HfO_2 and ZrO_2 by several researchers for the tetragonal to monoclinic transformation can be summarized as follows.

(i) The high-temperature tetragonal phase $P4_2nmc$ cannot be quenched at room temperature.
(ii) There is an abrupt change in the lattice parameters at the transformation. It is shown that HfO_2 and ZrO_2 are strongly anisotropic in thermal expansion, with the b axis exhibiting negligible expansion while the expansion is substantial for the a and c axes.
(iii) The transformation is associated with a volume expansion, a shear strain and micro-twinning.

The compressive properties of the low pressure phases of Hf and Zr dioxides have been studied by a number of experimental and theoretical works. Nevertheless, bulk moduli of the different phases has been found to cover a wide range of values [4, 6, 8]. Based on the pressure dependence of the Raman shifts and the observed similarities between the high-pressure phases of ZrO_2 and HfO_2, for the monoclinic (MI) phases of HfO_2, Jayaraman *et al* have proposed a value of 180 ± 20 GPa for the B_0 of HfO_2. Recently, based on the observation of Raman spectra and x-ray diffraction patterns under high pressures, Dessgreniers *et al* [4] determined a much higher value of B_0 for the MI phase: 284 ± 30 GPa (with $B_0' = 5 \pm 2$). For the other phases, the same authors determined the bulk moduli to be 281 ± 10 GPa (with $B_0' = 4.2 \pm 0.9$) for OI and 340 ± 10 GPa (with $B_0' = 2.6 \pm 0.3$) for OII. In the last phase, a higher bulk modulus 400 ± 100 GPa was estimated by a linear fit for pressures between 0 and 13 GPa [4]. On the other side, a much lower value of 145 GPa (with $B_0' = 5$) for $P2_1/c$ has been reported by Leger *et al* [10].

Theoretical works exist in the literature dealing with structural, vibrational, dielectric properties and pressure induced phase transformations of hafnia. In a systematic calculation of transition metal dioxides belonging to the subgroup IVa [18], it was concluded that the LMTO-ASA method can adequately represent the forbidden bandgap width and cohesive energy of HfO_2 in the cubic fluorite phase [18]. Recently, Lowther *et al* investigated the structural properties of HfO_2 and ZrO_2 using the *ab initio* pseudopotential-plane-wave (PPPW) PHI98 method [14]. In that work the calculations of bulk moduli and relative stability for the high pressure phases were presented. They showed the similarities between phases of ZrO_2 and HfO_2 and confirmed the low compressibilities of the cotunnite-type phases of both compounds. During the course of the present work, other first principles PPPW studies of structural, lattice vibrations and dielectric properties of the high-temperature phases [15] and phase transitions [17] were reported. These theoretical predictions show just a partial agreement with each other and with experiments.

Due to the still unexplained large experimental dispersion of the measured structural properties of the normal phase $P2_1/c$, as well as its excellent thermal and dielectric properties in relation with its use as basic constituent material in future sub-micrometric CMOS gate oxides, the interest in this compound is quite enhanced. More theoretical investigations using first principles alternative methods that use a flexible linear combination of atomic orbitals (LCAO) basis set for the description of valence state are then desirable, together with comparisons to experimental and previous theoretical assessments, in order to ascertain the expected accuracy of current DFT code. This is the purpose of this work. We present here a detailed study of the electronic structure, static and elastic properties (bulk moduli), and relative energies of the known phases as a function of the hydrostatic pressure. Electronic densities of states (DOSs), forbidden bandgaps, equilibrium structures and transition pressures for the transformations $P2_1/c \rightarrow Pbca$, $Pbca \rightarrow Pnma$ is presented. These results are tested with the basis set size and are compared with those obtained by other authors with pseudopotentials and plane waves (PPPWs) [14, 16, 7, 17] and with the LMTO-ASA method [18]. Because other superhard oxides show the modified fluorite structure $Pa3$ as well, we study here the possible occurrence of this phase, too.

2. Theory

The SIESTA code [20] is utilized in this work to calculate energies and atomic forces solving the quantum mechanical equation for the electrons with the density functional approach in the local density approximation (LDA) parametrized by Ceperley and Alder and the generalized gradient approach (GGA) by Perdew, Burke and Ernzerhof (PBE) for the electronic exchange

and correlation potential. The interactions between electrons and core ions are simulated with separable Troullier–Martins norm-conserving pseudopotentials. The basis set is constructed with pseudoatomic orbitals (PAOs) of the Sankey–Niklewsky type [21], generalized to include multiple-zeta decays and polarization functions which are used to represent the valence wavefunctions [22].

We have generated our own atomic pseudopotentials for both atoms, Hf and O, in the compound. In the case of the Hf atom, we found that it is not necessary to include the Hf 4f shell in the valence set to achieve reliable results even in the more demanding case of the volume collapse of the cotunnite phase (the atomic volume decreases by 13%). However, we found it is important to apply partial core correction in the Hf pseudopotential generation in order to accurately reproduce the equilibrium volume even with a single basis set. Thus, we generate the atomic Hf pseudopotentials using the [Xe $4f^{14}$]$5d^2 6s^2$ atomic configuration. The selected cut-off radii for our atomic pseudopotentials were for Hf 2.7, 2.9 and 2.25 au for the s, p and d components respectively, and for O 1.15 au for both the s and p channels and 0.8 au for both the d and f channels respectively.

In the context of the SIESTA approach the use of pseudopotentials imposes orbital basis sets adapted to the so-called pseudo-atomic orbitals (PAOs). They are used in the DFT solution of the atom together with the pseudopotential. The starting point for our basis sets is PAOs which are confined in a spherical potential well with infinite barrier boundary conditions. A single parameter that defines the confinement radius of different orbitals is called the orbital energy shift and is defined to be the increase of the energy of each l orbital when it is confined in such a finite sphere. It defines all orbital radii in a well balanced way and allows the systematic convergence of different physical quantities to the required precision (see [23–26]).

We systematically investigated the influence of these parameters on the total energies and derived structural properties like equilibrium lattice constants, bulk moduli and their derivatives in different high-density and high-temperature phases of the oxide. Also, the relative energies between phases were checked out and were compared upon change of the cut-off energies, and sizes of basis set. The quality of the uniform grid of points (the mesh) used to represent charge densities and potentials in real space is measured by the energy of the shortest plane wave that can be described with this grid, in analogy with plane wave calculation. After testing the normal phase with cut-off energies between 30 and 160 Ryd, and different basis sets, we found optimal values around 80 Ryd for 24-atom cells and 90 Ryd for 12-atom cells. All atoms were allowed to relax until atomic forces were less than 0.04 eV $Å^{-1}$. In the calculations of relative energies, to minimize differences in the total energies coming from the different size cells, with the exception of $P4_2nmc$, all calculations shown here were carried out with 24-atom cells, which is reached by duplicating the 12-atom cell along the a axis. In figure 1 are shown the unit cells of the studied phases, where each one is drawn with its original shape. Convergence studies carried out increasing the number of k-points showed that uniform grids between 16 and 28 k-points ($P21c$—16 kp, $Pbca$—20 kp, $Fm3m$—16 kp, $P4_2nmc$—20 kp, $Pnmc$—28 kp) were enough to obtain converged total energies E_t to about 1 meV/atom. The theoretical values of bulk moduli with different oxygen coordinations are here presented and compared with the available values found in the experimental literature.

3. Results and discussion

3.1. Electronic, static and structural properties

In this study the procedure used to find the combination of optimal basis set, $E_{cut-off}$, confinement energy and number of k-points which optimize efficiency and keeping accuracy

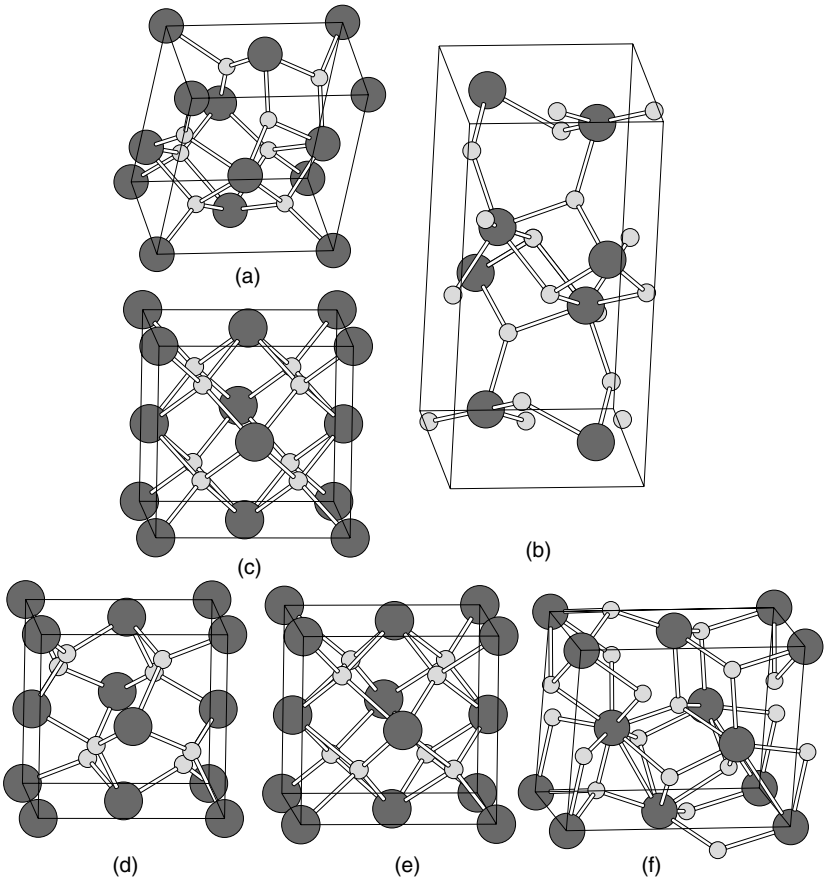

Figure 1. Unit cells of HfO_2 compounds at equilibrium volumes after the internal atomic positions were allowed to relax. Dark circles represent Hf atoms and small light grey circles represent the O atoms. Note the similarity between $Pa3$ and fluorite $Fm3m$ arrangements; however, the O atoms in $Pa3$ are placed very close to the centre of the triangles formed by three Hf atoms, while in the $Fm3m$ symmetry each O atom is placed at the centre of a tetrahedron. (a) $P2_1/c$; (b) $Pbca$; (c) $Fm3m$; (d) $Pa3$; (e) $P4_2nmc$; (f) $Pnma$.

under control was the following. First, we used a minimal basis set with larger confinement and then again a minimal basis set with lower confinement. This procedure was applied in a more robust basis set and checked with the previous SZ basis set. The test of convergence with respect to ΔE_{PAO}, number of k-points, sampling grid size (cut-off energy) etc was carried out in the normal phase. In figure 2 we illustrate the total energy curves corresponding to the normal $P2_1/c$ phase, using different basis sets: single ζ (SZ), single ζ polarized (SZP), double ζ (DZ) and double ζ polarized (DZP). They are shown here with two confinement energies ΔE_{PAO}, 40 and 70 meV, which are a compromise between precision and efficiency found in this calculation. The calculated equilibrium volumes for the 12-atom $P2_1/c$ cell (see figure 2) are found to be 135.8 Å^3 for the SZ-40 meV basis set, 134.7 Å^3 for SZ-70 meV, 136.8 Å^3 for SZP-40 meV, 137.5 Å^3 for SZP-70 meV, 136.2 Å^3 for DZ-40 meV, 137 Å^3 for DZ-70 meV, 135.1 Å^3 for DZP-40 meV and 135.5 Å^3 for DZP-70 meV Å^3, respectively, close to the experimental value, 138.2 Å^3 [4]. The fitted B_0 values corresponding to this normal phase, with different basis sets and using the two mentioned ΔE_{PAO} corresponding to the $E(V)$

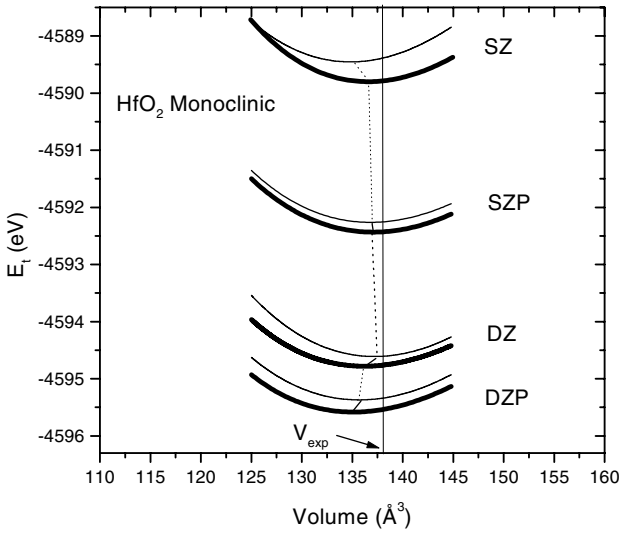

Figure 2. Total energy $E(V)$ of monoclinic HfO_2 calculated with SZ and DZ basis sets. Units of E_t in eV/(12-atom unit cell).

curves of figure 2, are 295 GPa for the SZ-40 meV basis set, 288 GPa for SZ-70 meV, 246 GPa for SZP-40 meV, 271 GPa for SZP-70 meV, 254 GPa for DZ-70 meV, 239 GPa for DZ-40 meV, 237 GPa for DZP-40 meV and 247 GPa for DZP-70 meV, respectively. In this case, the SZ value are close to the $B_0 = 284$ GPa measured by Desgreniers *et al* [4], while the DZ and DZP fits are close to the $B_0 = 233$ GPa given by Wang *et al* [12]. It is worth mentioning that execution times for runs with the 12 atoms $P2_1/c$ cell which include the relaxations of all atomic coordinates, axis lengths and the beta-angle, using $\Delta E_{PAO} = 70$ meV, are (in a 40 MFlops Linpack 400×400 machine) 7222 s for the SZ basis set, 22 395 s for SZP, 17 874 s for DZ and about 50 000 s for DZP. These runs include about 20–30 conjugate gradient steps which in turn include a total of 130–160 self-consistent-field steps. To have one idea about the impact of the localization parameter on the efficiency of the calculation, if ΔE_{PAO} is diminished to 40 meV, there appears an increase in the execution times of about 20%, while the increase of ΔE_{PAO} to 100 meV lowers the execution times by about 20%. This last value is more adequate to perform Order[N] calculations.

3.1.1. The use of double-ζ basis set. A systematic investigation was completed in the rest of the known phases of hafnia. The study shows that PAO functions with an imposed energy shift $\Delta E_{PAO} = 70$ meV, a double-ζ valence basis set together with the conjugated gradient method used for the optimization of internal atomic coordinates and cell parameters, are sufficient to obtain accurate equilibrium volumes V_0, lattice lengths a_i and equilibrium bulk moduli B_0 in correspondence with previous state-of-the-art *ab initio* PPPW assessments [14]. Figure 3 shows the total densities of states of the normal phase ($P2_1/c$) and those of the high-pressure and the high-temperature phases, calculated with this double-zeta decay, $\Delta E_{PAO} = 70$ meV. The bandgaps, defined to be the energy difference between the top of the valence band (where $e_{vb} = 0$ eV) and the bottom of the conduction band ($e_{cb} > 0$ eV) are found to be 3.54, 3.79, 2.85, 3.50, 3.93 and 3.32 eV for the phases $P2_1/c$, $Pbca$, $Pnma$, $Fm3m$, $P4_2nmc$ and $Pa3$ respectively. These bandgaps are in good agreement with recent theoretical calculations

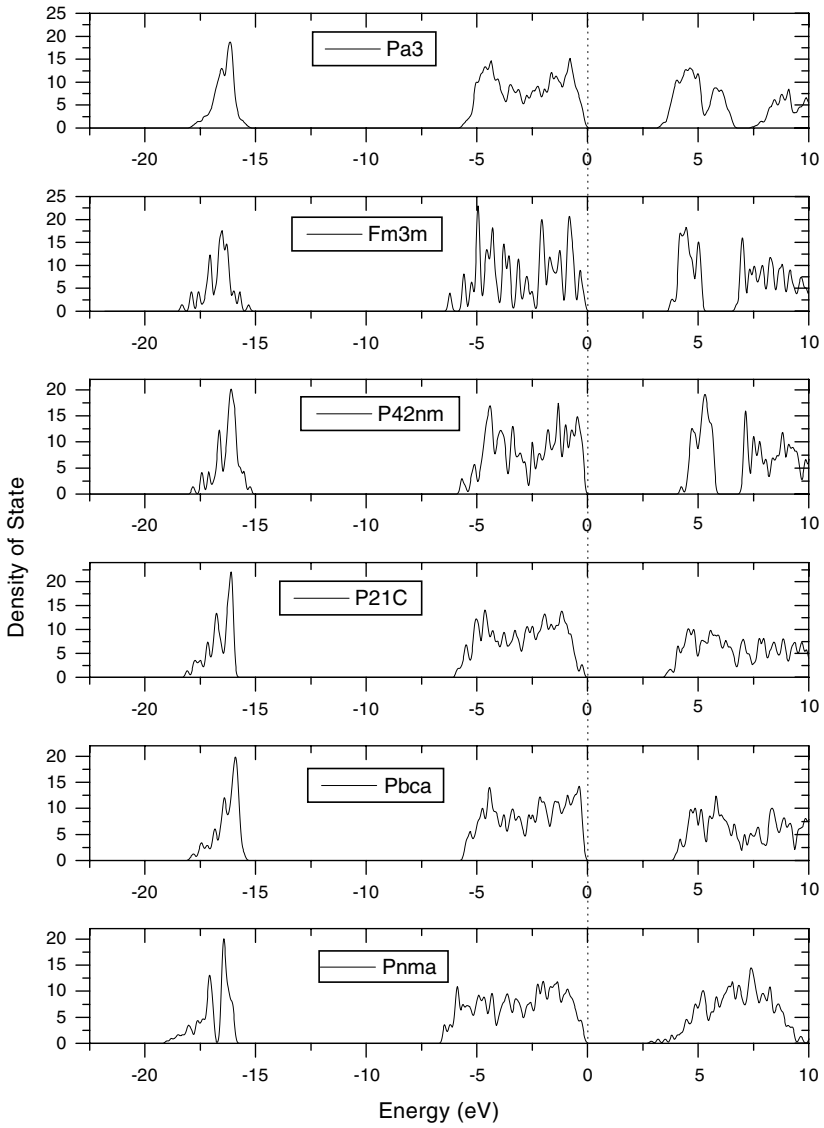

Figure 3. Total density of states of different phases of HfO_2 for DZ–LDA calculations, in units of states/unit-cell/spin/eV.

developed with the PPPW (CASTEP) method by Demkov [16], who found the values $E_g = 3.48$, 3.28 and 3.77 eV for $P2_1/c$, $Fm3m$ and $P4_2nmc$ respectively. More recently, Zhao *et al* [7] calculated the values 3.45, 3.75, 2.94, 3.15 and 3.84 eV for the phases $P2_1/c$, $Pbca$, $Pnma$, $Fm3m$ and $P4_2nmc$ respectively, which are again in close agreement with our calculated bandgaps (see table 1). The experimental value quoted in the literature is $E_g = 5.63$ eV [19].

Figure 4(a) shows theoretical total energy curves of the normal, high-temperature and high-pressure phases. Each point in the curve $E_t(V)$ is determined applying a target hydrostatic pressure. After the target pressure is applied, internal atomic coordinates as well as lengths and angles of the lattice vectors in the cell are released with molecular dynamics to minimize

Table 1. Theoretical bandgaps of the compounds studied here. E_g is in units of eV.

Phase	E_g^{th-SZ} (eV)[a]	E_g^{th-DZ} (eV)[a]	E_g^{th} (eV)[b]	E_g^{th} (eV)[c]
$P2_1c$ (monoclinic)	3.10	3.54	3.45	3.48
$Pbca$ (OI)	3.22	3.79	3.75	—
$Pnma$ (OII)	2.59	2.85	2.94	—
$Fm3m$ (cubic)	3.04	3.50	3.15	3.40
$P4_2nmc$ (tetrag)	3.25	3.8	3.84	3.77
$Pa3$	3.03	3.32	—	—

[a] Present work with LDA.
[b] Reference [15].
[c] Reference [16].

Table 2. Theoretical and experimental values corresponding to structural and elastic properties of HfO_2 in the $P2_1/c$ (monoclinic) phase. The volumes are related to the formula unit HfO_2. The calculated V_0, B_0 and B' were found by fitting the $E(V)$ curves to the Birch–Murnaghan equation of state. V_0 is in units of Å^3/molecule, while structural parameters a, b, c and β are in units of Å and degrees, respectively.

Method	V_0	B_0 (GPa)	B'	a	b	c	β
SIESTA (DZ)[a]	34.3	254	3	5.10	5.17	5.26	99.12
SIESTA (SZ)[a]	33.92	296	4.6	5.05	5.17	5.27	
PPPW (LDA)[h]	34.98	186	—	5.135	5.244	5.269	
PPPW (GGA)[h]	36.39	192	—	5.215	5.293	5.350	
PHI98[b]	34.56	251	4.4	5.12	5.17	5.29	99.25
VASP[c]	34.81	—	—	5.13	5.31	5.30	99.78
CASTEP[d]	33.92	—	—	5.08	5.19	5.22	99.77
Expt[e]	35.02	233	—	5.11	5.17	5.29	99.18
Expt[f]	34.57	185 ± 20	—	—	—	—	—
Expt[g]	34.91	284 ± 10	5 ± 2	—	—	—	—

[a] Present work.
[b] Reference [14].
[c] Reference [27].
[d] Reference [16].
[e] Reference [12].
[f] Reference [6].
[g] Reference [4].
[h] Reference [17].

interatomic forces. This procedure seems to be efficient and realistic since the application of an external constant pressure as a parameter not only mimics experiments under hydrostatic pressures but also does not impose—in theory—any restriction on the volume size and shape.

In tables 2–7 are shown the calculated equilibrium cell parameters: lattice axis lengths, cell angle (of $P2_1/c$), equilibrium volume cell (normalized to the formula unit), and elastic properties under hydrostatic pressures represented by the bulk modulus B_0 and its pressure derivative B_0'. These values are here compared with previous *ab initio* calculations [14, 17, 27, 16] and measurements performed with the diamond anvil cell technique (DAC) and with the x-ray diffraction technique under pressure [12, 6, 4] and temperature [28].

As said, in the case of the normal phase we found that our calculated V_0 is in good agreement with previous reliable LDA calculations and with recent experimental assessments: $V_0^{DZ-70\ meV} = 34.3$ Å^3/molecule is slightly below the reported experimental V_{exp} values, 35.02 Å^3/molecule [12], 34.57 Å^3/molecule [6] and 34.91 Å^3/molecule [4]. Jayaraman *et al* [6] suggested a value of $B_0 = 185$ GPa, much smaller than $B_0 = 233$ GPa given by Wang

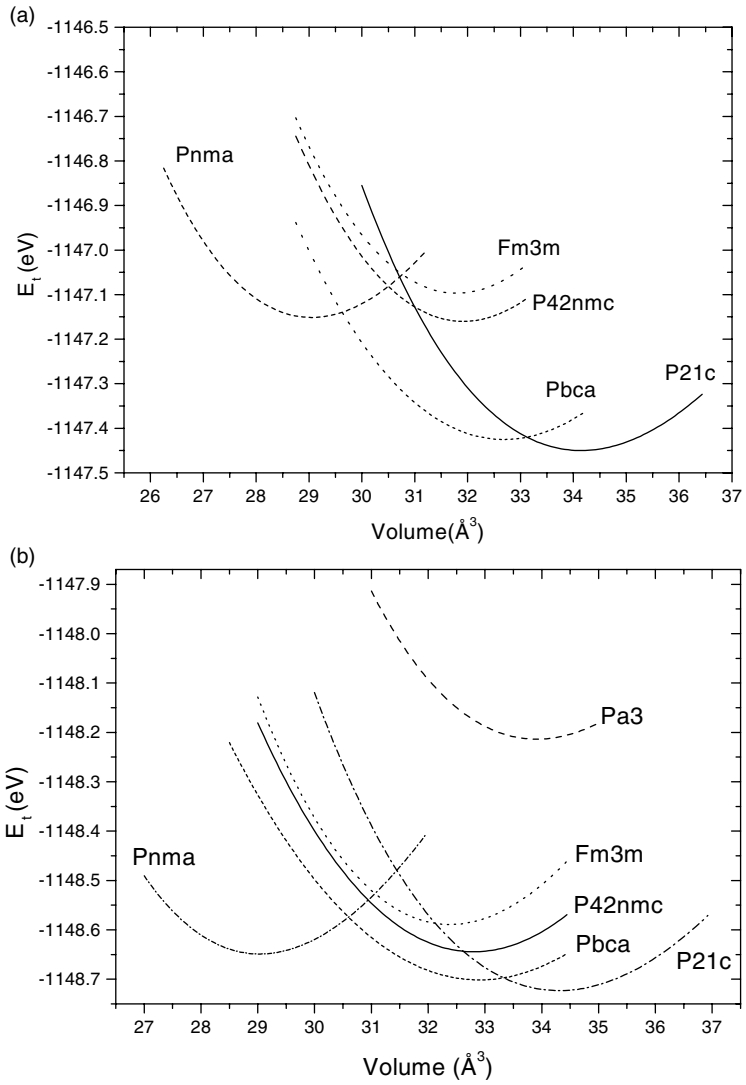

Figure 4. Theoretical total energies per formula unit corresponding to HfO_2 as a function of the cell volume, phase and basis set: (a) shows calculations with LDA and SZ basis sets while (b) shows calculations performed with LDA and DZ basis sets.

et al [12] and $B_0 = 284$ GPa measured by Desgreniers *et al* [4]. The lower B_0 value estimated in [6] was deduced from the comparison between ZrO_2 and HfO_2, which show almost identical molar volumes, structural correspondence and high-pressure behaviour. This low value could be associated with the presence of porosity in the samples, which significantly lower the bulk modulus of the ceramic as shown in the review of Wang *et al* [12]. In this respect our value $B_0^{\prime \mathrm{DZ}-70\ \mathrm{meV}} = 254$ GPa is between these two last measurements as well as in agreement with the $B_0 = 251$ GPa calculated by Lowther *et al* [14], with the PPPW and LDA approach. Other very recent PPPW calculations by Kang *et al* [17] obtained $B_0 = 186$ GPa with the LDA approach and $B_0 = 192$ GPa using the GGA approach, both of which fit better with the mentioned estimation by Jayaraman *et al*. Unfortunately, other research using VASP and

Table 3. Theoretical and experimental values corresponding to structural and elastic properties of HfO_2 in the $Pbca$ (OI) phase. The volumes are related to the formula unit HfO_2. V_0 is in units of $Å^3$/molecule, while structural parameters a, b and c are in units of Å and degrees, respectively.

Method	V_0	B_0 (GPa)	B'	a	b	c
SIESTA (DZ)[a]	32.87	244	4	10.05	5.22	5.04
SIESTA (SZ)[a]	32.68	289	2	9.96	5.19	5.01
PPPW (LDA)[g]	33.67	251	—	10.079	5.266	5.075
PPPW (GGA)[g]	35.04	221	—	10.215	5.324	5.154
PHI98[b]	34.46	256	4.15	10.22	5.31	5.08
Expt[c]	33	—	—	10.014[a]	5.22	5.05
Expt[d]	—	220	—	—	—	—
Expt[e]	32.02	281 ± 10	4.2 ± 0.9	—	—	—
Expt[f]	33.25	—	—	—	—	—

[a] Present work.
[b] Reference [14].
[c] Reference [12].
[d] Reference [28].
[e] Reference [4].
[f] Reference [6].
[g] Reference [18].

Table 4. Theoretical and experimental values corresponding to structural and elastic properties of HfO_2 in the $Pnma$ (OII) phase. The volumes are related to the formula unit HfO_2. V_0 is in units of $Å^3$/molecule, while structural parameters a, b and c are in units of Å and degrees, respectively.

Method	V_0	B_0 (GPa)	B'	a	b	c
SIESTA (DZ)[a]	28.95	328	4.5	3.26	6.39	5.56
SIESTA (SZ)[a]	29.05	335	4	3.25	6.44	5.55
PPPW (LDA)[g]	29.89	295	—	3.293	6.531	5.57
PPPW (GGA)[g]	31.18	252	—	3.353	6.606	5.629
PHI98[b]	30.65	306	4.57	3.35	6.68	5.48
Expt[c]	29.65	—	—	—	—	—
Expt[d]	30.19	—	—	3.37	6.46	5.55
Expt[e]	—	312	—	—	—	—
Expt[f]	30.58	340 ± 10	—	3.347	6.503	5.62

[a] Present work.
[b] Reference [14].
[c] Reference [6].
[d] Reference [9].
[e] Reference [28].
[f] Reference [4].
[g] Reference [18].

CASTEP codes did not quote this parameter. Differences between our theoretical equilibrium lattice constants and recent experimental values measured at the ambient temperature with the x-ray diffraction technique by Desgreniers *et al* [4] are lower than 1% for $P2_1/c$, $Pbca$ and $Pnma$ phases, which is very good for a heavy metal oxide theoretical assessments using the LDA approach. Tables 2–7 show the agreement between the primitive lattice vector lengths here calculated, and the experimental values reported of these phases. Note as well that the calculated beta angle of the monoclinic cell, 99.18°, is very accurate and almost coincides with the most accurate experimental value cited in the review of Wang *et al* [12]. In the case of the $P4_2nmc$ high-temperature phase, the departure of the equilibrium volumes and parameter cells

Table 5. Theoretical and experimental values corresponding to structural and elastic properties of HfO_2 in the $P4_2nmc$ phase. The volumes are related to the formula unit HfO_2. V_0 is in units of $Å^3$/molecule, while structural parameters a, b and c are in units of Å and degrees, respectively.

Method	V_0	B_0 (GPa)	B'	a	b	c
SIESTA (DZ)[a]	32.8	265 ± 30	4	5.03	5.04	5.18
SIESTA (SZ)[a]	31.9	381 ± 4	2	5.02	5.02	5.06
CASTEP[b]	32.5	—	—	3.56	3.56	5.11
VASP[c]	33.12	—	—	5.06	5.06	5.18
Expt[d]	35.11	—	—	5.15	5.15	5.295
Expt[e]	35.65	—	—	5.175	5.175	5.325

[a] Present work.
[b] Reference [16].
[c] Reference [27].
[d] Reference [12] at 1760 °C.
[e] Reference [12] at 2000 °C.

Table 6. Theoretical and experimental values corresponding to structural and elastic properties of HfO_2 in the $Fm3m$ phase. The volumes are related to the formula unit HfO_2. V_0 is in units of $Å^3$/molecule, while structural parameters a, b and c are in units of Å and degrees, respectively.

Method	V_0	B_0 (GPa)	B'	a	b	c
SIESTA (DZ)[a]	32.36	341.8 ± 9	5.8	5.06	5.06	5.06
SIESTA (SZ)[a]	31.8	391 ± 5	2	5.03	5.03	5.03
PPPW (LDA)[g]	32.89	289	—	5.086	5.086	5.086
PPPW (GGA)[g]	34.10	257	—	5.148	5.148	5.148
PHI98[b]	33.94	280	4.63	5.14	5.14	5.14
VASP[c]	32.49	—	—	5.07	5.07	5.07
CASTEP[d]	32.01	—	—	5.04	5.04	5.04
Expt[e]	33.35	—	—	5.11	5.11	5.11
Expt[f]	33.95	—	—	5.14	5.14	5.14

[a] Present work.
[b] Reference [14].
[c] Reference [27].
[d] Reference [16].
[e] Reference [12] at 1600 °C.
[f] Reference [12].
[g] Reference [18].

Table 7. Theoretical and experimental values corresponding to structural and elastic properties of HfO_2 in the $Pa3$ phase. The volumes are related to the formula unit HfO_2. V_0 is in units of $Å^3$/molecule, while structural parameters a, b and c are in units of Å and degrees, respectively.

Method	V_0	B_0 (GPa)	B'	a	b	c
SIESTA[a]	33.92	319.5 ± 20	5	5.14	5.14	5.14
PPPW[b]	36.38	262	4.6	5.26	5.26	5.26

[a] Present work.
[b] Reference [14].

is higher than the other cases measured at ambient temperature. In table 8 we summarize the theoretical relative total energies of the $Pbca$, $Pnma$, $Fm3m$, $P4_2nmc$ and $Pa3$ phases with respect to the monoclinic $P2_1/c$ phase for SZ and DZ basis sets and compare with previous GGA and LDA calculations. These differences are extracted from the minima of the total energy curves of each phase as a function of volume, shown in figure 4.

Table 8. Theoretical relative total energies per formula unit (fu) relative to the $P2_1/c$ phase of several studied compounds studied. E_t is in units of eV/formula unit.

Phase	E_t^{SZ} (eV)[a]	E_t^{DZ} (eV)[a]	E_t (eV)[b]	E_t (eV)[c]	E_t (eV)[d]	E_t (eV)[e]
$P2_1c$ (monoclinic)	0	0	0	0	0	0
$Pbca$ (OI)	0.0275	0.02	0.06	0.005	0.034	3.79
$Pnma$ (OII)	0.31	0.07	0.06	0.100	0.282	—
$Fm3m$ (cubic)	0.39	0.16	0.17	0.118	0.169	0.24
$P4_2nmc$ (tetrag)	0.30	0.08	—	0.095	0.135	0.16
$Pa3$	—	0.51	—	—	—	

[a] Present work LDA.
[b] Reference [14] LDA.
[c] Reference [17] LDA.
[d] Reference [17] GGA.
[e] Reference [27] GGA.

3.1.2. The use of minimal single-ζ basis set. While the DZ basis set together with $\Delta E_{PAO} = 70$ meV allows us to obtain equilibrium volumes and structural properties in accordance with earlier PPPW results; SZ together with $\Delta E_{PAO} = 40$ in turn allows us to calculate equilibrium volumes and bulk moduli in fair agreement with DZ and considerably reduce execution times. Moreover, it improves relative energies between phases. This subject will be discussed in the next subsection. We will discuss for the moment the structural and equilibrium properties, with numerical values shown in tables 2–7. The normal phase (table 2) has an equilibrium volume for SZ equal to 33.92 Å^3/molecule. This value is slightly bigger than the 34.3 Å^3/molecule calculated with DZ and lower than the experimental values 35.02 Å^3/molecule [12], 34.57 Å^3/molecule [6] and 34.91 Å^3/molecule [4]. The bulk modulus results in 296 GPa, which is about 16% greater than the calculated one with DZ and with the PHI98 code, and 4% higher than the highest experimental value available for this phase, 284 GPa, found by Desgreniers *et al* [4]. For the $Pbca$ phase, the calculated bulk modulus $B = 289$ GPa is close to the value $B = 281$ GPa found by Desgreniers *et al* [4], while the theoretical equilibrium volume value and primitive axis lengths are underestimated in 1% and <0.4% respectively, with respect to experiments [4]. In the $Pnma$ phase, the value $B = 335$ GPa is in very good agreement with the reported $B = 340$ GPa by Desgreniers *et al* [4]. The equilibrium volume, 29.05 Å^3/molecule, is very close to our $V_0 = 28.95$ Å^3/molecule calculated with DZ (see table 4) and 5% below to the experimental equilibrium value of 30.58 Å^3/molecule found by Desgreniers *et al* [4]. The axis lengths have an average departure of 1% with respect to experiments [4]. The bulk moduli of the high temperature polymorphs have values of $B = 391$ and 381 GPa for the $Fm3m$ and $P4_2nmc$ phases, respectively. The B_0 ($Fm3m$) is much larger than the theoretical 341, 289 and 280 GPa, calculated with SIESTA-DZ (present work), by Kang *et al* and by Lowthers *et al*, respectively (see table 6) and the $B_0(P4_2nmc)$ is again much larger than the 265 GPa calculated with SIESTA-DZ. It seems that these two cases for the high-temperature, eightfold coordinated phases have the largest disagreement with other calculations. However, the conclusion remains open because of the absence of experimental information in this regard.

At this point it is worth mentioning that our calculations do not include any dilatation due to lattice vibrations. This correction seem to be very important in the range of equilibrium temperatures at normal pressures which goes from 1600° to 2600°. In the case of $Fm3m$, the phase is stable at temperatures from 2600° to 2800°, the value at which the material becomes liquid. Due to lattice anharmonicities, the inclusion of lattice vibrations at high temperatures should increase all equilibrium volumes and one can get better agreement with the experiment. However, these corrections exceed the aim of the present work and they are not included here.

3.2. Transition pressures

The transition pressure is usually calculated from the Gibbs free energy $G = H - TS$, where the enthalpy is defined as $H = E + PV$ [13], where E here is the electronic total energy, P is the hydrostatic pressure and V is the cell volume. Since all calculations are carried out without including ion vibrations, this assumption is equivalent to assuming that the system is at $T = 0$ temperature and neglecting zero-point vibrations. Then the transition pressure is determined by equating the enthalpies of both phases at the pressure at which the phase transition occurs.

In figure 5(a) we show the relative enthalpy of $Pbca$, $Pnma$, $Fm3m$ and $P4_2nmc$ phases with respect to the $P2_1/c$ one, using the SZ minimal basis set. The transition pressure from the normal to the intermediate phase ($P2_1/c \rightarrow Pbca$) is estimated to be about 3 GPa, which is close to the reported experimental transition pressures at which the full transition occurs: 2.6 GPa [8], 4 GPa [4] and 4.3 GPa [11]. The phase $Pbca$ is theoretically more stable from 3 GPa until pressures around 12 GPa, the value at which the transition to $Pnma$ theoretically starts. It can be noted that the enthalpy difference of $Pbca$ with respect to $P2_1/c$ has a low departure as the pressure increases, and even at pressures of 12 GPa the enthalpy difference $\Delta H(Pbca - P2_1/c)$ does not exceed 0.5 eV per formula unit, and both phases can coexist. This can explain the experimental evidence of a sluggish transition. For pressures in excess of 12 GPa, $Pnma$ becomes more stable, but its relative enthalpy is in turn more pressure dependent than the $Pbca$ phase. In the same graph we see that both the high temperature phases $P4_2nmc$ and $Fm3m$ have relative enthalpies higher than the normal and high-pressure phases, indicating theoretically that they are not stable, as found in experiments. The above interpretation is only valid using the minimal basis set. When the double ζ is used instead, the mentioned pressures drop to 1 and 2.3 GPa for the transitions $P2_1/c \rightarrow Pbca$ and $Pbca \rightarrow Pnma$ respectively (see figure 5(b)). We think that this diminution is due to the underestimation of energy differences between phases of the same compound found previously in other LDA assessments [14, 17]. Since the double-ζ basis set is more complete, one can think that density gradient terms in the cell are better represented and therefore energy differences of polymorphs should have more systematic errors. In the single-ζ description, the charge density is smoother and more convenient for the LDA description. This fact was tested here in calculations performed with the same minimal basis set but using the GGA-PBE approach: the energy difference between $P2_1/c$ and $Pnma$ phases hardly changes with respect to LDA. However, since DZ basis set calculations give more detailed charge densities, they are more sensitive to LDA systematic errors (the effect of homogeneity of electron densities on energy terms using LDA and GGA was studied in detail, using pseudopotentials and plane waves in HfO_2, by Kang *et al* [17]). Our calculations in 12-atom cells with DZ-GGA enlarge energy differences $E(Pnma - P2_1/c)$ to about 0.9 eV instead of the 0.28 eV obtained with DZ–LDA. As found in [17], on going from the normal phase to cotunnite, the electron distribution becomes more homogeneous, and the energy lowering due to GGA is larger in $P2_1/c$. This fact increases the transition pressure.

3.2.1. Effects of pressure on structural parameters. In figure 6 we show the variations of the unit cell parameters, a, b and c, the β angle and the volume corresponding to the $P2_1/c$ cell as a function of the target pressure, calculated with the DZ basis set. The b axis shows small slope from 0 to 12 GPa and almost no variation beyond 12 GPa. The variation of the a axis with pressure shows a clear break at a value close to 12 GPa, which is also seen in the c axis and to a lesser degree in the cell volume dependence. This behaviour was also noted in XRD experiments [8] and associated with the onset of a sluggish phase transition where traces of the monoclinic phase were identified at 20 GPa. On the other hand, in the orthorhombic type-II $Pnma$ phase, all lattice parameters are linear and practically insensitive to pressure in

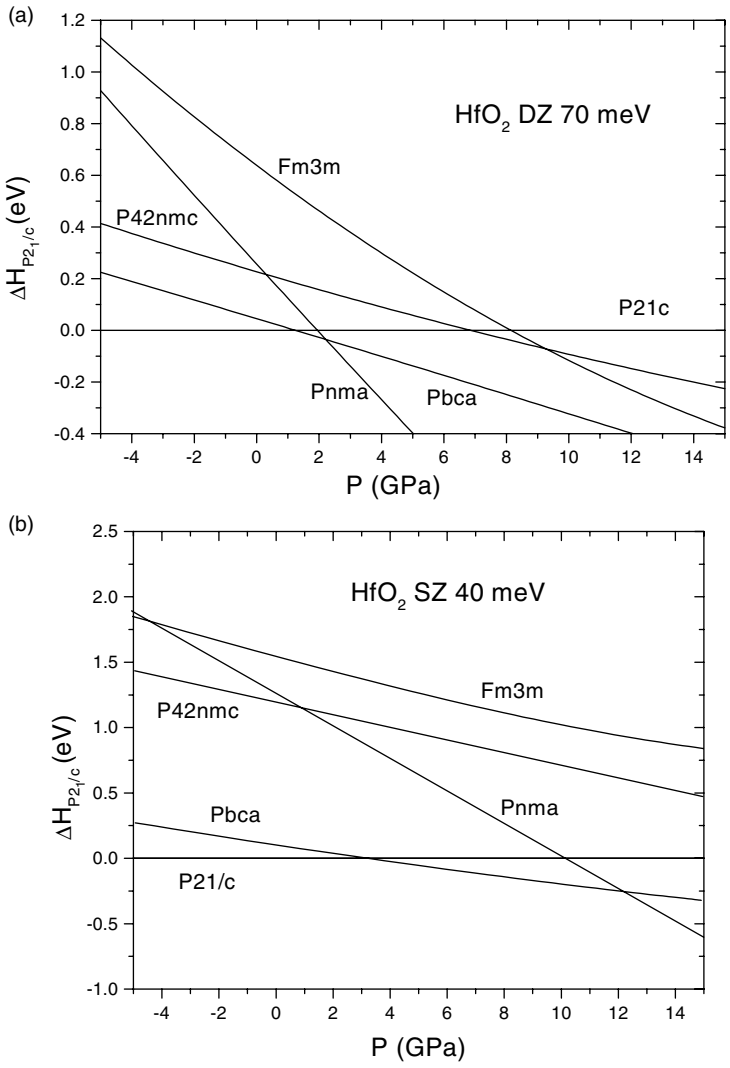

Figure 5. Relative enthalpies to the normal phase, for $Pbca$, $Pnma$, $P4_2nmc$ and $Fm3m$ phases respectively according to the basis set and normalized to 12 atoms. In (a) are shown LDA calculations with SZ and in (b) with the DZ basis set.

the range from 0 to 10 GPa, as evidence of high hardness. This computer experiment should be interesting to carry out using another constant pressure approach like the Parrinello–Rahman method, for instance.

4. Conclusions

Since similar studies on this compound using PPPW approaches have been carried out, the aim of this work is to quantify the accuracy and efficiency of the SIESTA code in HfO_2 polymorphs (using a minimal basis set, in turn giving a chance to deal with order[N] systems). We applied the following procedure: first we used a minimal basis set of larger confinement and then the results are checked against minimal basis set calculations but with lower confinement. Then

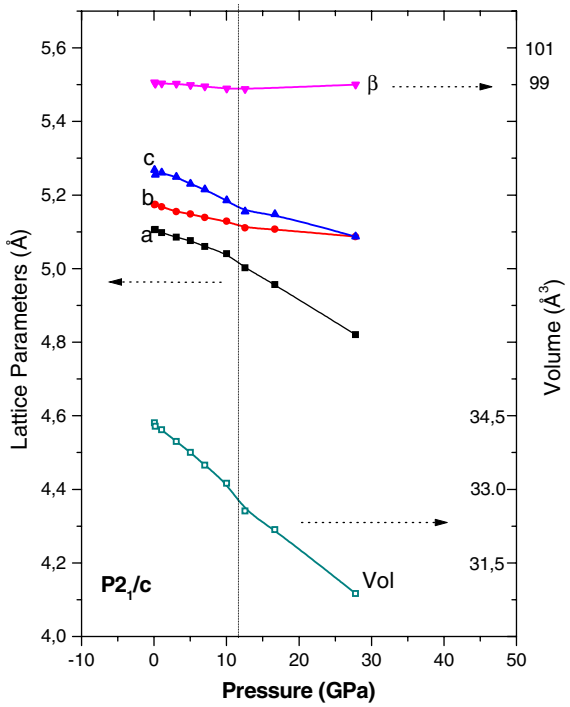

Figure 6. Calculated lattice cell parameters and cell volume as a function of the numerically applied hydrostatic pressure for $P2_1/c$.

(This figure is in colour only in the electronic version)

more robust double-ζ polarized basis sets are utilized and these results are checked against the previous one. The new finding is that a minimal basis set that uses confinement radius (represented by the shift of the localized orbital) equal to 40 meV is enough to describe with realism phase transitions under pressure of polymorphs without contradicting any experimental evidence. We have found that LDA together with the minimal basis set (SZ) and confinement radius improve relative enthalpies when they are compared to double-ζ basis set calculations. As a consequence, the calculated pressure transitions between the normal phase and OI and OI $\rightarrow$ OII are in better agreement with experiments than the DZ–LDA combination. This is because LDA is a better prescription for slowly varying charge density representations such as the SZ approach. We predicted the bulk moduli of the high-temperature phases $Fm3m$ and $P4_2nmc$ and studied the possible existence at high temperatures of the phase with $Pa3$ symmetry. The bulk moduli, which are numerically fitted to the Birch–Murnaghan equation of state, show increasing rigidity of the lattices when one passes from the low-pressure phase $P2_1/c$, to the higher one $Pbca$ and $Pnma$. The same can be concluded for the $Fm3m$ and the $Pa3$ phases. The calculated bulk modulus of the highly coordinated, toughened ceramic $Pnma$ phase of HfO_2 is 328 GPa, in agreement with the value of 340 GPa measured by Desgreniers *et al*, confirming its possible usage as hardened material. In this respect, we developed another separate work related to the elastic properties of $Pnma$ crystals with the NFP-LMTO method and their polycrystals using the theories of Voigt and Reuss and found that the bulk modulus is very close to the present values found with SIESTA. In this regard, we assign this agreement to the core corrections included in our Hf pseudopotentials.

In the ordering of high-temperature phases, we found the following sequence of phases as the temperature is increased: $P4_2nmc$, $Fm3m$ and $Pa3$ phases. This fact does not contradict experimental evidence or previous theoretical calculations.

In the case of the SZ minimal basis set, comparing the enthalpy $H(p)_{Pbca}$ with respect to the homologous $H(p)_{P21/c}$, we have found at 3 GPa the transition pressure of the $P2_1/c \rightarrow Pbca$ transformation, a value which lies in the range of experimental measurements, 2.6–4.3 GPa. Following the same procedure but applied to the transition $Pbca \rightarrow Pnma$, P_t is now 12 GPa, close to the pressures at which the cotunnite phase ($Pnma$) was found experimentally to appear.

In summary, the prescriptions we found here are the following.

(1) Electronic, equilibrium and elastic properties are very well accounted for in HfO_2 polymorphs with the LDA–DZ approach giving quality comparable with other state of the art PPPW *ab initio* calculations;
(2) If transition pressures calculated from relative enthalpies are looked for, the LDA–SZ–40 meV prescription is more adequate since it gives comparable results to those obtained using PPPW and GGA approaches.

Based on these findings as a final remark we conclude that if LDA is to be used to describe HfO_2, then it is better with a single-ζ basis set. With this prescription, the SIESTA code seems to be a promising tool in future studies at nanometric scale of this or similar high-hardness metallic oxides.

Acknowledgments

We are grateful to J E Lowther for providing useful Information and to Pablo Ordejon (IMAB-Barcelona) and Jarek Dabrowski (IHP-Franfurt/Oder) for stimulating and valuable discussions. We also thank the Institute for High Performance Microelectronics, Frankfurt/Oder, Germany, for hospitality and partial support. This work was partially supported by Secretaria de Ciencia y Tecnica of the Universidad Nacional del Nordeste, Argentina, project No 653.

References

[1] Lee J C 2000 *4th Annual Topical Research Conf. on Reliability (Sematech and SMSI Public Meetings, Stanford University, October 2000)*
[2] Espladio M J, Avalle L V and Macagno V A 1997 *Electrochem. Record* **42** 1315
[3] Platt C L, Dieny B and Berkowitz A E 1996 *Appl. Phys. Lett.* **69** 2291
[4] Desgreniers S and Lagarec K 1999 *Phys. Rev.* B **59** 8467 (up to 70 GPa)
[5] Liu L G 1980 *J. Phys. Chem. Solids* **41** 331
[6] Jayaraman A, Wang S Y, Sharma S K and Ming L C 1993 *Phys. Rev.* B **48** 9205
[7] Zhao X and Vanderbilt D *Proc. 2002 MRS Fall Mtg* vol 745, p 7.2.1
[8] Adams D M, Leonard S and Russell D R 1991 *J. Phys. Chem. Solids* **52** 1181 (up to 20 GPa)
[9] Haines J, Leger J L, Hull S, Petitet J P and Pereira T O 1997 *J. Am. Ceram. Soc.* **80** 1910
[10] Leger J M, Atouf A, Tomaszewski P E and Pereira A S 1993 *Phys. Rev.* B **48** 93
[11] Arashi H 1992 *J. Am. Ceram. Soc.* **75** 844
[12] Wang J, Li H P and Stevens R 1992 *J. Mater. Sci.* **27** 5397 (review of hafnia)
[13] Borg R J and Dienes G J 1992 *The Physical Chemistry of Solids* (New York: Academic)
[14] Lowther J E, Dewhurst J K, Leger J M and Haines J 1999 *Phys. Rev.* B **60** 14485
[15] Zhao X and Vanderbilt D 2002 *Phys. Rev.* B **65** 233106
[16] Demkov A A 2001 *Phys. Status Solidi* b **226** 57
[17] Kang J, Lee E-C and Chang K J 2003 *Phys. Rev.* B **68** 54106
[18] Medvedeva N I, Zhukov V P, Khodos M Ya and Gubanov V A 1990 *Phys. Status Solidi* b **160** 517

[19] Samsonov G V 1980 *Oxide Handbook* (London: Akademik)
[20] Soler J M, Artacho E, Gale J, Garca A, Junquera J, Ordejón P and Sanchez-Portal D 2002 *J. Phys.: Condens. Matter* **14** 2745
[21] Sankey O F and Niklewski D J 1989 *Phys. Rev.* B **40** 3979
[22] Artacho E, Sanchez-Portal D, Ordejón P, Garcia A and Soler J M 1999 *Phys. Status Solidi* b **215** 809
[23] Ordejón P, Artacho E and Soler J M 1996 *Phys. Rev.* B **53** R10441
[24] Ordejón P, Artacho E and Soler J M 1996 *Mater. Res. Soc. Symp. Proc.* **408** 85
[25] Sánchez Portal D, Ordejón P, Artacho E and Soler J M 1997 *Int. J. Quantum Chem.* **65** 453
[26] Sánchez Portal D 1998 *Doctoral Thesis* Universidad Autonoma de Madrid
[27] Foster A S, Lopez Gejo F, Shluger A L and Nieminen R M 2002 *Phys. Rev.* B **65** 174117
[28] Ohtaka O, Fukui H, Kunisada T, Fujisawa T, Funakoshi K, Utsumi W, Irifune T, Kuroda K and Kikegawa T 2001 *J. Am. Ceram. Soc.* **84** 1369